References

[1] Cornish, J. J., "Some Aerodynamic and Operational Problems of STOL Aircraft With Boundary-Layer Control," *Journal of Aircraft*, Vol. 2, March-April 1965, pp. 78-86.

[2] Hoerner, S., *Fluid-Dynamic Drag*, published by author, Midland Park, N. J., 1958.

[3] Schlichting, H., *Boundary Layer Theory*, McGraw-Hill, New York, 1960.

[4] Roberts, S. C. et. al., "XV-11A Description and Preliminary Flight Test," USAAVLABS Tech. Rept. 67-21, May 1967.

[5] Roberts, S. C., "The Marvel Report, Part E – Solution to the Problem of Obtaining Two-Dimensional Boundary Layer Data on the Variable-Camber High-Lift Wings of the Marvelette," U.S. Army TRECOM Tech. Rept. 65-16, May 1965.

[6] Gregory, N. and Walker, W. S., "Wind-Tunnel Tests on the NACA 63A009 Aerofoil with Distributed Suction Over the Nose," ARC R&M No. 2900, Sept. 1952.

[7] Dannenburg, R., Gambucci, B., and Weiberg, J., "Perforated Sheets as a Porous Material for Distributed Suction and Injection," NACA TN 3669, April 1956.

[8] Abbott, I. and Doenhoff, A., *Theory of Wing Sections*, Dover, New York, 1959.

Dynamic Blade Row Compression Component Model for Stability Studies

W.A. Tesch* and W.G. Steenken†

General Electric Company, Cincinnati, Ohio

Nomenclature

A = area
$A_{I\beta}$ = area normal to relative flow
C = axial velocity
C_T = absolute tangential velocity
IGV = inlet guide vane
L = volume length
M = Mach number
N = wheel speed
P = static pressure
P_d = dynamic pressure ($P_T - P$)
P_T = total pressure
S = entropy
V = volume
W = physical flow rate
a = acoustic velocity
q = kinetic pressure ($\frac{1}{2}\rho v^2$)
r = pitch-line radius
v = velocity
t = time

Introduction

PREDICTING the stability characteristics of turbofan engines when subjected to a wide variety of steady and unsteady inlet flow distortions remains a continuing problem that must be solved successfully if airframe/engine integration is to occur with no inlet/engine compatibility problems. To date, the engine developer has relied upon historical data and empirical correlations. However, such approaches, although providing visibility at the inlet/engine interface, do not lend themselves to understanding the impact of compressor design variables when trying to achieve a solution to potential or existing stability problems.

As a first step in developing a compression system stability analysis tool, an operationally verified compression component stability model has been developed, which accurately reproduces experimentally determined speed lines and accurately predicts the associated surge point. The following discussion which is taken from Ref. 1 describes this model, the manner in which a solution is achieved, and the results obtained by simulating an eight-stage compressor.

Formulation of Model

This analysis begins with the complete set of nonlinear partial differential equations known as the equations of change[2] which describe the transport processes within a fluid. These equations have been integrated once over an arbitrary control volume of the flow system to obtain the "macroscopic balances." It should be noted that the energy equation was combined with one of the thermodynamic *Tds* relationships[3] prior to integration. The "macroscopic balances" for mass, momentum, and energy, respectively, are reproduced here in the form that they are used in the dynamic model:

$$\frac{\partial \bar{\rho}}{\partial t} = \frac{1}{V}(W_1 - W_2) \tag{1}$$

$$\frac{\partial \bar{W}}{\partial t} = \frac{1}{L}[W_1 C_1 - W_2 C_2 + P_1 A_1 - P_2 A_2 - P_M(A_1 - A_2) + F_B] \tag{2}$$

$$\frac{\partial \overline{\rho S}}{\partial t} = \frac{1}{V}[W_1 S_1 - W_2 S_2 + S_F] \tag{3}$$

The variables subscripted by 1 and 2 on the right-hand side of the equations refer to quantities at the inlet and exit stations of the control volume, respectively. The left-hand side of the equation represents time derivatives of volume averaged properties. With reference to Fig. 1, it is seen that P_M represents the mean pressure acting on the lateral area of the fluid, and F_B is the blade force acting upon the fluid. The term S_F, the total rate of irreversible conversion of mechanical to internal energy, in the case of this model represents the entropy production caused by blade row losses.

Equations (1-3), other than being applicable to quasi-one-dimensional flows in finite volumes without heat transfer, properly describe the state of a fluid in motion. In order for a solution to be obtained, it is necessary to supply the caloric and thermal equations of state and expressions for P_M, S_F, and F_B.

The mean pressure term represents the mean of the static pressure distribution acting on the lateral surface of the blade row and free volumes. The complication introduced by this term results from the fact that rigorous determination of its value requires invoking the momentum equation and can lead to over constraint of the system of equations. The mean pressure for blade row volumes is determined from the empirical relationship where

$$P_M = (2P_L + P_S)/3 \tag{4}$$

P_L is the larger of the volume inlet or exit station static pressures, and P_S is the smaller of the volume inlet or exit station static pressures. This empirical relationship was developed by examining an exact calculation of the mean pressure in a compression component with no losses and assuming that the relationship developed for lossless blade rows would remain valid for the actual case where blade row losses are taken into account. The mean pressure for free

Presented as Paper 76-203 at the AIAA 14th Aerospace Sciences Meeting, Washington, D. C., Jan. 26-28, 1976; submitted March 23, 1976; revision received April 29, 1977.

Index categories: Airbreathing Propulsion; Nonsteady Aerodynamics; Computational Methods.

*Engineer, Stability and Installation Aerodynamics, Aircraft Engine Group.

†Manager, Stability and Installation Aerodynamics, Aircraft Engine Group. Associate Fellow AIAA.

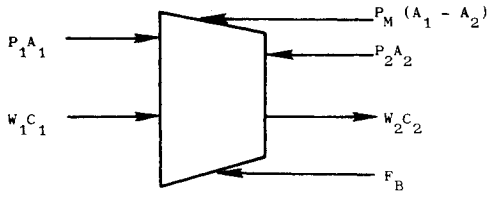

Fig. 1 Forces acting on control volume.

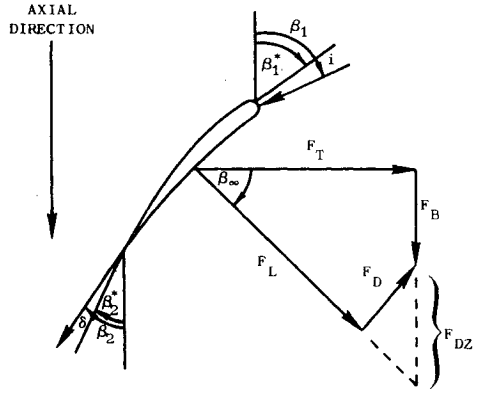

Fig. 2 Blade geometry, flow geometry, and force acting on fluid.

volumes is based upon a steady isentropic flow derivation which uses a polynomial representation in Mach number. Subsequent integration of the truncated polynomial results in an expression of the form

$$P_M = \frac{(P_{T_1} + P_{T_2})}{2(M_2 - M_1)} [C_1 (M_2 - M_1) + C_2 (M_2^2 - M_1^2) + C_3 (M_2^3 - M_1^3) + C_4 (M_2^4 - M_1^4) + C_5 (M_2^5 - M_1^5)] \quad (5)$$

The entropy production term S_F can be written as

$$S_F = \bar{W}\ell_n \frac{(P'_{T_2}/P'_{T_1})_{\text{ideal}}}{(P'_{T_2}/P'_{T_1})_{\text{actual}}} \quad (6)$$

where the ideal relative total-pressure ratio which accounts for the change in pitch line radius[4] from the entrance of a rotor blade row to its exit is written as

$$\left(\frac{P'_{T_2}}{P'_{T_1}}\right)_{\text{ideal}} = \left\{1 + \frac{\gamma - 1}{2} M_T^2 \left[1 - \left(\frac{r_1}{r_2}\right)^2\right]\right\}^{\gamma/(\gamma-1)} \quad (7)$$

M_T is equal to the ratio of the blade row exit pitch line wheel speed to the inlet relative stagnation velocity of sound ($2\pi Nr_2/a'_{T_1}$). In the case of a stator, the ideal relative total-pressure ratio is equal to one. The actual relative total pressure requires knowledge of the relative total-pressure coefficient which is defined as

$$\bar{\omega}' = \frac{(P'_{T_2})_{\text{ideal}} - (P'_{T_2})_{\text{actual}}}{P'_{T_1} - P_1} \quad (8)$$

Equation 8 can be rewritten in the form

$$\left(\frac{P'_{T_2}}{P'_{T_1}}\right)_{\text{actual}} = \left(\frac{P'_{T_2}}{P'_{T_1}}\right)_{\text{ideal}} - \bar{\omega}' \left\{1 - \left[\frac{1}{1 + [(\gamma-1)/2](M'_1)^2}\right]^{\gamma/(\gamma-1)}\right\} \quad (9)$$

Hence, Eqs. (7) and (9), when substituted into Eq. (6) provide complete definition of the entropy production term.

The relative total-pressure loss coefficient is an input which is a function of the incidence angle and is determined from steady clean-inlet-flow data which are obtained by throttling the compression component at constant corrected speed.

The blade force acting on the fluid is determined by resolving the forces that act upon a blade. Figure 2 illustrates the forces under consideration. The blade force is related to the inlet and exit flow angles and the change in angular momentum through the blade row. The inlet flow angle (β_1) is equal to the sum of the inlet metal angle (β_1^*) and the incidence angle (i). The exit flow angle (β_2) is equal to the sum of the exit metal angle (β_2^*) and the deviation angle (δ). The deviation angle is determined from the same data set as the relative total-pressure loss coefficient and is input as a function of the blade incidence angle. The direction of the lift vector (F_L) is assumed to be the average of the inlet and exit air angles plus a small correction angle β_c which is discussed later in this section. It is given as

$$\beta_\infty = (\beta_1 + \beta_2)/2 + \beta_c \quad (10)$$

The drag acting on the fluid can be related to the relative total-pressure loss coefficient ($\bar{\omega}'$) through the expression

$$F_D = \bar{\omega} \frac{P'_1}{P'_{T_1}} \frac{P'_{d1}}{q'_1} A_{1\beta} q_1 \quad (11)$$

where the prime indicates the relative flow frame of reference. Hence, the axial blade force can be written as

$$F_B = F_T \tan\beta_\infty - F_{DZ} \quad (12)$$

where $F_{DZ} = F_D[\cos(\beta_i - \beta_\infty)]/\cos\beta_\infty$ and the tangential blade force acting on the fluid (F_T) can be derived from a general expression for the change of angular momentum[5] through a blade row.

$$F_T = \frac{2(r_2 W_2 C_{T_2} - r_1 W_1 C_{T_1})}{r_1 + r_2} + V \frac{d}{dt}(\bar{\rho} C_T) \quad (13)$$

The first term on the right-hand side of Eq. (13) is one variant of the steady flow Euler Turbine Equation. The second term represents the force associated with the rate of accumulation of angular momentum within a blade row volume.

In the case of steady flow, it is possible to obtain a solution to a compression component flow problem using either Eqs. (1) and (2) ("force balance") or Eqs. (1) and (3) ("energy balance"). The energy balance always gives the correct solution, that is, it matches the results of steady-state stage stacking procedures. The force balance solution typically results in less pressure rise than actually takes place. This fact is a result of the assumed direction (β_∞) of the lift force vector. Hence, a small correction angle (β_c) is determined by comparison of the two solutions and is added to the assumed lift direction vector. In general, the lift direction correction angle is a nearly linear function of incidence angle and has a magnitude that is less than a few degrees. The steady-state force balance solution also usually is used to initialize the dynamic model for the start of computation. At this point it is useful to discuss the manner in which a model of a compression component is modeled from some measurement plane upstream of the compressor face to a known downstream boundary condition such as a choke plane at the turbine nozzle diaphragm. Each blade row is assigned a volume with a rotor volume length extending from the upstream stator trailing edge to the downstream stator leading edge. The ducting upstream of the compressor face to the measurement plane, the compressor discharge, and the combustor are divided into blade-free volumes whose lengths are chosen to be commensurate with the longest blade row volume. Hence, the ultimate frequency response of the model

is essentially determined by the length of the longest blade row volume.

A time marching technique is employed to solve Eqs. (1-3). This technique is based upon a Taylor series expansion of three independent volume averaged flow properties at time t to estimate volumes of the flow properties at time $t+\Delta t$. The flow properties under consideration in this model are the volume averaged density, physical flow rate, and density-specific entropy product. Solution of the equations is straightforward and will be illustrated for one variable, the volume-averaged density. The Taylor series correct to second order for volume averaged density in a given volume can be written as

$$\bar{\rho}(t+\Delta t)=\bar{\rho}(t)+\frac{\partial\bar{\rho}(t)}{\partial t}\Delta t+\frac{\partial^2\bar{\rho}(t)}{\partial t^2}\frac{(\Delta t)^2}{2} \tag{14}$$

where $\bar{\rho}(t)$ is established by the initial conditions or from a previous time step and $\partial\bar{\rho}(t)/\partial t$ can be obtained from Eq. (1). Differentiation of Eq. (1) results in

$$\frac{\partial^2\bar{\rho}(t)}{\partial t^2}=\frac{1}{V}\left(\frac{\partial W_1}{\partial t}-\frac{\partial W_2}{\partial t}\right) \tag{15}$$

Examination of the right-hand side of the equation reveals that it is composed of time derivatives of station variables. Hence, Eq. (2), per se, cannot be used to establish their values. Therefore, it is at this point that one resorts to interpolation to obtain the necessary station values from the volume-averaged properties of the two adjacent volumes. Similarly, this technique can be used for the remaining two variables and can be continued from one time step to the next until the transient dies out or stationary behavior is obtained, either case being dependent upon the imposed boundary conditions.

Results

The clean-inlet-flow map of an eight-stage compressor has been simulated. This compressor with a hub-to-tip radius ratio of 0.476 has a flapped IGV which is scheduled as a function of corrected speed, but biased by engine face total temperature (T_{T_2}). Stages 3, 4, and 5 are bled at the casing wall midway in a stator passage. They are controlled in the same manner as the IGV, since they are ganged together with the IGV. The clean-inlet-flow data were obtained during an engine test. All of the losses within a stage were assigned to the rotor blade rows. Also, the rotor rows had varying deviation angles whereas the stators had constant deviation angles. Handling blade characteristics in this manner does not represent a limitation of the model, but rather is a limitation of the available test data. The geometry included in the model extended from an instrumentation plane upstream of the IGV's where a constant total-pressure and total-temperature boundary condition was imposed to the turbine nozzle diaphragm where throttling of the compressor was controlled by ramping the flow function ($W\sqrt{T}/P$). A comparison of the 80, 87, 94, and 100% corrected speed lines and the surge line

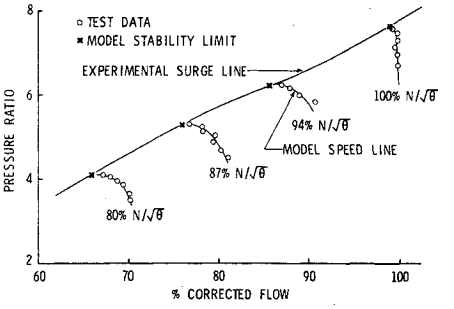

Fig. 3 Eight-stage compressor clean-inlet-flow map.

obtained from test data with the model simulations is shown in Fig. 3. As was expected, the agreement between test and simulated speed lines is excellent.

Considerable effort was expended to determine a criterion that would indicate reliably that the stable operating range had been exceeded. Many flow variables were examined as a function of time to determine if any exhibited marked changes as the region of expected instability was approached. It was found that a marked change was shown by the ratio of the derivative of the volume-averaged physical flow with respect to the derivative of the flow at the exit plane where the throttling boundary condition was being imposed. When this ratio exceeded a value of 2 in all blade rows and the throttling was terminated, the model would not settle into steady-state conditions, but rather the flow would continue to decrease until the model encountered numerical problems. The value of 2 was found to be independent of ramping rate. The location of this aerodynamic instability always coincided with the experimentally determined surge line. This stability criterion represents the fact that the internally generated disturbances are growing faster than the disturbance imposed by the boundary conditions. Hence, it is akin to a change in sign of eigenvalues for any boundary value problem as one moves from a region where disturbances are attenuated to a region where disturbances propagate.

Acknowledgment

The results presented in this paper were obtained under National Aeronautics and Space Administration Contract NAS3-18526 with the Lewis Research Center Engine Research Branch, Cleveland, Ohio.

References

[1] Tesch, W. A. and Steenken, W. G., "Dynamic Blade Row Compression Component Model for Stability Studies," AIAA Paper 76-203, Washington, D. C., Jan. 26-28, 1976.

[2] Bird, R. B., Stewart, W. E., and Lightfoot, E. N., *Transport Phenomena*, Wiley, New York, 1960.

[3] Obert, E. F., *Concepts of Thermodynamics*, McGraw-Hill, New York, 1960.

[4] Johnsen, I. A. and Bullock, R. O. (Eds.), "Aerodynamic Design of Axial-Flow Compressors," NASA SP-36, revised 1965.

[5] Shepherd, D. G., *Elements of Fluid Mechanics*, Harcourt, New York, 1965.